

# Interactions of Charged Porphyrins with Nonionic Triblock Copolymer Hosts in Aqueous Solutions

Christian A. Steinbeck, Niklas Hedin, and Bradley F. Chmelka\*

Department of Chemical Engineering, University of California,  
Santa Barbara, California 93106

Received June 24, 2004. In Final Form: August 27, 2004

The extent and locus of solubilization of guest and self-assembling surfactant host molecules in aqueous solutions are influenced by a variety of hydrophobic and hydrophilic interactions, as well as by more specific interactions between the various species present. By using a combination of two-dimensional heteronuclear  $^{13}\text{C}\{^1\text{H}\}$  NMR correlation experiments with pulsed-gradient NMR diffusion and proton cross-relaxation measurements, the locations and distributions of porphyrin guest molecules have been established unambiguously with respect to the hydrophobic and hydrophilic moieties of a triblock copolymer species in solution. The interactions of tetra(4-sulfonatophenyl)porphyrin with the poly(propylene oxide) (PPO) and the poly(ethylene oxide) (PEO) segments of amphiphilic PEO–PPO–PEO triblock copolymer species have been measured as functions of solution conditions, including temperature and pH. The porphyrin/PEO–PPO–PEO interactions are established to be selective and adjustable according to the different temperature-dependent hydrophilicities or hydrophobicities of the PEO and PPO triblock copolymer components. Furthermore, such interactions influence the self-assembly properties of the block-copolymer amphiphiles in solution by stabilizing molecular porphyrin/PEO–PPO–PEO complexes well above the critical micellization temperature of the triblock copolymer species under otherwise identical conditions.

## Introduction

Nonionic block-copolymer aggregates have been used as hosts for organic guest molecules in systems with a wide range of potential applications,<sup>1</sup> including drug delivery,<sup>2</sup> separations,<sup>3</sup> and solid-state optoelectronic devices.<sup>4,5</sup> For each of these systems and applications, a molecular-level understanding of the conditions and factors that influence key guest–host interactions is desirable, particularly in heterogeneous systems. An important step to understanding such interactions is to characterize in detail the guest interaction sites, as well as the dynamics and mechanisms of molecular association. In heterogeneous host systems, however, this often presents a difficult challenge, as a number of different local environments exist. In self-assembled micellar solutions, for example, these include solvent, micellar cores, and coronas, as well as smaller surfactant aggregates and fully solubilized surfactant molecules (so-called unimers). Depending on the relative interaction energies, guest species can often be selectively solubilized in any of these locally distinct nano-environments. The mobilities of guest components may differ in the different regions, with dynamic molecular exchange possible among the different environments. Furthermore, the presence of the guest species may also influence the micellization behavior of the host.

The bulk micellization behaviors of triblock copolymers of poly(ethylene oxide) (PEO) and poly(propylene oxide)

(PPO) have been studied extensively.<sup>4–28</sup> Their properties in aqueous solution depend on the relative fractions and lengths of the PEO and PPO moieties, which can be varied, so that they represent a versatile group of water-soluble

- (6) Alexandridis, P.; Holzwarth, J. F.; Hatton, T. A. *Macromolecules* **1994**, *27*, 2414–2425.
- (7) Wanka, G.; Hoffmann, H.; Ulbricht, W. *Macromolecules* **1994**, *27*, 4145–4159.
- (8) Mcdonald, C.; Wong, C. K. *J. Pharm. Pharmacol.* **1974**, *26*, 556–557.
- (9) Rassing, J.; Attwood, D. *Int. J. Pharm.* **1982**, *13*, 47–55.
- (10) Zhou, Z. K.; Chu, B. *Macromolecules* **1988**, *21*, 2548–2554.
- (11) Brown, W.; Schillen, K.; Almgren, M.; Hvidt, S.; Bahadur, P. *J. Phys. Chem.* **1991**, *95*, 1850–1858.
- (12) Mortensen, K.; Pedersen, J. S. *Macromolecules* **1993**, *26*, 805–812.
- (13) Jain, N. J.; Aswal, V. K.; Goyal, P. S.; Bahadur, P. *J. Phys. Chem. B* **1998**, *102*, 8452–8458.
- (14) Jain, N. J.; Aswal, V. K.; Goyal, P. S.; Bahadur, P. *Colloid Surf. A* **2000**, *173*, 85–94.
- (15) Jain, N. J.; George, A.; Bahadur, P. *Colloid Surf. A* **1999**, *157*, 275–283.
- (16) Malmsten, M.; Lindman, B. *Macromolecules* **1992**, *25*, 5446–5450.
- (17) Jorgensen, E. B.; Hvidt, S.; Brown, W.; Schillen, K. *Macromolecules* **1997**, *30*, 2355–2364.
- (18) Armstrong, J. K.; Chowdhry, B. Z.; Snowden, M. J.; Leharne, S. A. *Langmuir* **1998**, *14*, 2004–2010.
- (19) Bahadur, P.; Li, P. Y.; Almgren, M.; Brown, W. *Langmuir* **1992**, *8*, 1903–1907.
- (20) Bahadur, P.; Pandya, K.; Almgren, M.; Li, P.; Stilbs, P. *Colloid Polym. Sci.* **1993**, *271*, 657–667.
- (21) Pandya, K.; Lad, K.; Bahadur, P. *J. Macromol. Sci. Pure Appl. Chem.* **1993**, *A30*, 1–18.
- (22) Armstrong, J.; Chowdhry, B.; Mitchell, J.; Beezer, A.; Leharne, S. *J. Phys. Chem.* **1996**, *100*, 1738–1745.
- (23) Alexandridis, P.; Athanassiou, V.; Hatton, T. A. *Langmuir* **1995**, *11*, 2442–2450.
- (24) Lad, K.; Bahadur, A.; Pandya, K.; Bahadur, P. *Indian J. Chem. A* **1995**, *34*, 938–945.
- (25) Marinov, G.; Michels, B.; Zana, R. *Langmuir* **1998**, *14*, 2639–2644.
- (26) Hecht, E.; Mortensen, K.; Gradzielski, M.; Hoffmann, H. *J. Phys. Chem.* **1995**, *99*, 4866–4874.
- (27) Lad, K.; Bahadur, A.; Bahadur, P. *Tenside, Surfactants, Deterg.* **1997**, *34*, 37–42.
- (28) Su, Y.; Wang, J.; Liu, H. *J. Phys. Chem. B* **2002**, *106*, 11823–11828.

\* Author to whom correspondence should be addressed.

- (1) Forster, S.; Plantenberg, T. *Angew Chem. Int. Ed.* **2002**, *41*, 689–714.
- (2) Rosler, A.; Vandermeulen, G. W. M.; Klok, H. A. *Adv. Drug Delivery Rev.* **2001**, *53*, 95–108.
- (3) Chu, B. J.; Liang, D. H. *J. Chromatogr. A* **2002**, *966*, 1–13.
- (4) Yang, P. D.; Wirnsberger, G.; Huang, H. C.; Cordero, S. R.; McGehee, M. D.; Scott, B.; Deng, T.; Whitesides, G. M.; Chmelka, B. F.; Buratto, S. K.; Stucky, G. D. *Science* **2000**, *287*, 465–467.
- (5) Wirnsberger, G.; Yang, P. D.; Scott, B. J.; Chmelka, B. F.; Stucky, G. D. *Spectrochim. Acta A* **2001**, *57*, 2049–2060.

nonionic macromolecular surface-active agents.<sup>6,7</sup> One of the most striking properties of these triblock copolymer systems is the strong temperature dependence of their phase behaviors in aqueous solutions. In particular, it has been shown<sup>8</sup> that, at low temperatures ( $\sim 15^\circ\text{C}$ ), both the PEO and PPO blocks are significantly hydrated and, below a critical micellization temperature, the triblock copolymer species are present in solution mainly as individual unimers. With increasing temperature, the PPO moieties become increasingly hydrophobic and the amphiphilic character of the triblock copolymer increases, leading to the formation of micellar aggregates in aqueous solutions at a critical micellization temperature (CMT).<sup>9–12,28</sup> As the temperature is increased further, the local environments in both the micellar PPO cores and the surrounding PEO coronas become increasingly hydrophobic and, above a critical solution temperature, both copolymer blocks become insoluble and the solution macroscopically phase separates.

The inclusion of various additives or guests has been shown to affect significantly the aggregation behavior of PEO–PPO triblock copolymers in aqueous solution. Detailed investigations have focused on the effects of the addition of various salts, which tend to decrease the CMT.<sup>9,13–21</sup> The addition of organic solvents<sup>22</sup> and nonelectrolytes<sup>21–23</sup> has also been studied, with some additives (e.g., urea, methanol, and ethanol) acting to raise the CMT, while others (e.g., butanol) were found to lower it. Furthermore, the incorporation of conventional surfactants can suppress PEO–PPO copolymer micellization.<sup>24–27,29</sup> The micellization behaviors of PEO–PPO triblock copolymers are thus affected by a variety of solution parameters, notably temperature and composition. These lead to their versatile properties that are exploited in a large number of industrial applications,<sup>30</sup> including uses in detergents, inks, lubricants, and cosmetics. PEO–PPO–PEO triblock copolymers have more recently been introduced for use in various medical applications<sup>31–33</sup> and as structure-directing agents in the syntheses of mesostructured inorganic–organic hybrid materials.<sup>4,34</sup>

Given the breadth of applications for PEO–PPO triblock copolymer systems, the choices of potential guest species and processing conditions are vast and general strategies for controlling the loading and distribution of guest species associated with the copolymer host are required. In aqueous solutions, the locations of the guest species are typically inferred by considering their hydrophobic or hydrophilic characters or are predetermined by covalently binding the guest species to a specific block of the triblock copolymer host.<sup>35</sup> In the absence of other dominating interactions, guest species that interact strongly and attractively with either or both of the PEO and PPO triblock copolymer segments will be solubilized by the triblock copolymer host. In the absence of such attractive interactions, a hydrophilic molecule will be mainly solubilized in the aqueous region surrounding the triblock copolymer unimers or micelles, due to the entropic penalties associated with unimer complexation or solu-

bilization in the confined micellar coronas and because fewer water molecules are available in such associations for the formation of hydrogen bonds. Conversely, a hydrophobic molecule will be solubilized mainly in the hydrophobic core of the micelles to minimize interactions with surrounding water molecules. For a real system, numerous possible interactions need to be considered and the locus of solubilization depends on which interactions dominate under the specific solution conditions. The strong and differing temperature-dependences of the hydrophilic/hydrophobic characters of the PEO and PPO triblock copolymer segments in PEO–PPO systems consequently provide a means of balancing site-specific molecular interactions with hydrophilic/hydrophobic effects to thereby control the locus of guest–host interactions.

The free base of water-soluble tetra(4-sulfonatophenyl)porphyrin (TPPS<sub>4</sub>) was chosen as a promising candidate for measuring and controlling the distribution of guest species in aqueous PEO–PPO–PEO solutions. The four sulfonate groups of the porphyrin impart appreciable hydrophilicity to the guest molecules, while the complexing capability of the central macrocycle provides strong attractive interactions with the triblock copolymer.<sup>36</sup> In addition, porphyrins are technologically important guest species that have found uses in a number of medical applications, including use as photo- and radiosensitizers<sup>37</sup> and as magnetic-resonance-imaging contrast agents.<sup>38</sup> Furthermore, porphyrins tend to exhibit significant nonlinear optical properties<sup>39</sup> due to the large, conjugated  $\pi$ -electron systems associated with their central macrocycle. This makes them interesting for a variety of optical applications, including optically limiting protective coatings,<sup>40</sup> dye-sensitized solar cells,<sup>41,42</sup> and a range of applications in telecommunications and data storage/retrieval.<sup>43</sup>

The interactions of different porphyrins with various surfactant solution systems have been studied extensively,<sup>36,44–52</sup> although the focus has been principally on their interactions with ionic surfactants. For such ionic systems, micellization and solubilization behaviors at fixed surfactant concentrations are mainly affected by ionic strength. Solubilization studies have therefore focused on the effects of pH and variations in ion composition and

(29) Contractor, K.; Bahadur, P. *Eur. Polym. J.* **1998**, *34*, 225–228.

(30) Alexandridis, P.; Hatton, T. A. *Colloid Surf. A* **1995**, *96*, 1–46.

(31) Kabanov, A. V.; Batrakova, E. V.; Alakhov, V. Y. *Adv. Drug Delivery Rev.* **2002**, *54*, 759–779.

(32) Kabanov, A. V.; Batrakova, E. V.; Alakhov, V. Y. *J. Controlled Release* **2002**, *82*, 189–212.

(33) Kabanov, A. V.; Batrakova, E. V.; Meliknubarov, N. S.; Fedoseev, N. A.; Dorodnich, T. Y.; Alakhov, V. Y.; Chekhonin, V. P.; Nazarova, I. R.; Kabanov, V. A. *J. Controlled Release* **1992**, *22*, 141–157.

(34) Zhao, D. Y.; Feng, J. L.; Huo, Q. S.; Melosh, N.; Fredrickson, G. H.; Chmelka, B. F.; Stucky, G. D. *Science* **1998**, *279*, 548–552.

(35) Nagarajan, R. *Polym. Adv. Technol.* **2001**, *12*, 23–43.

(36) Vermathen, M.; Louie, E. A.; Chodosh, A. B.; Ried, S.; Simonis, U. *Langmuir* **2000**, *16*, 210–221.

(37) Ali, H.; van Lier, J. E. *Chem. Rev.* **1999**, *99*, 2379–2450.

(38) Schwert, D. D.; Davies, J. A.; Richardson, N. *Top. Curr. Chem.* **2002**, *221*, 165–199.

(39) Kadish, K. M., K. M. S.; Guillard, R., Eds.; *The Porphyrin Handbook*; Academic Press: New York, 1999.

(40) Melosh, N. A.; Scott, B. J.; Steinbeck, C. A.; Hayward, R. C.; Davidson, P.; Stucky, G. D.; Chmelka, B. F. *J. Phys. Chem. B* **2004**, *108*, 11909–11914.

(41) Wamser, C. C.; Kim, H. S.; Lee, J. K. *Opt. Mater.* **2003**, *21*, 221–224.

(42) Wohrle, D.; Meissner, D. *Adv. Mater.* **1991**, *3*, 129–138.

(43) Kobayashi, T., Ed. *Organic and Polymer Materials for Nonlinear Optics*; Taylor and Francis: London, 1990.

(44) Corsini, A.; Herrmann, O. *Talanta* **1986**, *33*, 335–339.

(45) Gandini, S. C. M.; Yushmanov, V. E.; Borissevitch, I. E.; Tabak, M. *Langmuir* **1999**, *15*, 6233–6243.

(46) Gandini, S. C. M.; Yushmanov, V. E.; Tabak, M. *J. Inorg. Biochem.* **2001**, *85*, 263–277.

(47) Hioka, N.; Chowdhary, R. K.; Chansarkar, N.; Delmarre, D.; Sternberg, E.; Dolphin, D. *Can. J. Chem.* **2002**, *80*, 1321–1326.

(48) Kadish, K. M.; Maiya, B. G.; Araullomcadams, C. *J. Phys. Chem.* **1991**, *95*, 427–431.

(49) Kadish, K. M.; Maiya, G. B.; Araullo, C.; Guillard, R. *Inorg. Chem.* **1989**, *28*, 2725–2731.

(50) Maiti, N. C.; Mazumdar, S.; Periasamy, N. *J. Phys. Chem.* **1995**, *99*, 10708–10715.

(51) Maiti, N. C.; Mazumdar, S.; Periasamy, N. *J. Phys. Chem. B* **1998**, *102*, 1528–1538.

(52) Monti, D.; Venanzi, M.; Cantonetti, V.; Borocci, S.; Mancini, G. *Chem. Commun.* **2002**, 774–775.

concentration. By monitoring changes in the absorption spectrum, it has, for example, been demonstrated that, by altering the pH, the interactions of an amphiphilic porphyrin derivative could be changed to favor the micellar cores or the outer surfaces of cationic micelles.<sup>53</sup> In contrast to studies focusing on ionic strength and pH, few temperature-dependent studies have been performed, in part because of the secondary role that temperature often plays in ionic surfactant solutions. In addition, the focus of these studies has been mainly on the temperature dependence of the solubilization capacity of the host system (i.e., the amount of guest molecules that can be solubilized) rather than on where guest species are located within the host micelles or the types of interactions present.<sup>54</sup> In nonionic surfactant solutions, such as the aqueous solutions of PEO-PPO triblock copolymers considered here, temperature tends to play an important role on the micellization and solubilization behaviors of such guest-host systems.

A molecular-level understanding of the temperature-dependent interactions between guest and host species under different solution conditions is therefore important for controlling their respective distributions and dynamics. Such information is typically sought from optical measurements (e.g., absorption and fluorescence spectroscopy), which reflect the different local environments experienced by the guest species. In many cases, however, such changes in the absorption or fluorescence properties of the guest species may be too weak or difficult to observe, so that the dye interactions and distributions cannot be accurately established. In addition, separate light-scattering experiments are typically necessary to provide information about the aggregation properties and, thus, the associated phase behaviors of these systems. Nuclear magnetic resonance (NMR) spectroscopy is a powerful means for quantitatively correlating the effects of different molecular and macroscopic variables on the structures and dynamics of host-guest species present in solution.<sup>55</sup> Two-dimensional (2D) NMR correlation techniques, in particular, provide enhanced spectral resolution that enables interactions among different species to be established on molecular-length scales. Complementary pulsed-gradient NMR measurements of diffusion coefficients probe longer micrometer-length scales and are sensitive to molecular aggregation behaviors. Diffusion coefficients can be correlated with the size (e.g., unimers versus micelles) of a species present in solution, and in many cases, it is possible to quantify exchange dynamics between different aggregation states.

Here, molecular and micellar structures and dynamics are investigated for an aqueous PEO-PPO-PEO triblock copolymer solution (pH = 11) containing TPPS<sub>4</sub> guest species. In particular, it is demonstrated for the first time that the loci of interactions of guest species associated with a nonionic surfactant copolymer can be measured and changed in a controllable way by variations in temperature, as established unambiguously by 2D NMR. Furthermore, small dye-triblock copolymer complexes are shown to be stabilized at temperatures well above the CMT of the binary water-triblock copolymer solution. The combined application of pulsed-gradient diffusion NMR and multidimensional heteronuclear correlation NMR techniques yields detailed insights into the molec-

ular processes and interactions that are responsible for these effects.

## Experimental Section

**Materials.** The porphyrin dye, tetra(4-sulfonatophenyl)porphyrin (TPPS<sub>4</sub>, Frontier Scientific), the poly(ethylene oxide)-poly(propylene oxide)-poly(ethylene oxide) triblock copolymer, EO<sub>20</sub>-PO<sub>70</sub>-EO<sub>20</sub> (Pluronic P123, BASF), deuterated water (D<sub>2</sub>O 99.9%, Sigma Aldrich), deuterium chloride (DCl 99.9%, Sigma Aldrich), and sodium deuterioxide (NaOD 99.9%, Sigma Aldrich) were used as received. Aqueous triblock copolymer solutions were prepared by adding cold D<sub>2</sub>O (5 °C) to P123 to obtain a concentration of 10 mM P123 and were stirred until the solutions were optically clear. The samples were then sonicated for 15 min, after which the pH (here, reflecting the concentration of deuterons, rather than protons) was adjusted to 11 through the addition of NaOD. The samples were then refrigerated at 5 °C overnight to equilibrate. The TPPS<sub>4</sub>-containing samples were prepared in a similar manner, but a calculated amount of NaOD (~75% of the total amount required to obtain a pH 11 solution) was added to the deuterated water to facilitate dissolution of the dye. After each solution was sonicated and equilibrated overnight, the pH was adjusted to a final value of 11 through the addition of further NaOD. All samples were allowed to equilibrate for at least 2 days before measurements were taken. Samples containing 10 mM P123, 10 mM TPPS<sub>4</sub>, and 10 mM in both P123 and TPPS<sub>4</sub> were prepared.

**NMR Methods and Analyses.** All NMR experiments were conducted on a Bruker AVANCE DMX-500 spectrometer equipped with a triple-gradient probehead with an inverse-detection-coil geometry using 5-mm sample tubes and solution volumes of 400  $\mu$ L. For all experiments, the samples were allowed to equilibrate at the desired temperature for at least 30 min prior to measurement; experiments that were repeated at the same temperature, but reached by a temperature change in the opposite direction, yielded identical results. Assignments of the various resonances were based on a combination of single-pulse <sup>1</sup>H NMR spectra and gradient-selected heteronuclear single-quantum coherence (HSQC) <sup>1</sup>H{<sup>13</sup>C} NMR spectra,<sup>56,57</sup> acquired using globally optimized alternating-phase rectangular pulse <sup>13</sup>C decoupling (GARP)<sup>58</sup> during acquisition. No internal standards were added to the sample because of the large propensity of TPPS<sub>4</sub> to bind to various substances that could have interfered with the measurements.<sup>59</sup> Solution-phase <sup>1</sup>H NMR spectra were therefore referenced to the <sup>1</sup>H signal ( $\pm 0.05$  ppm) from residual water<sup>60</sup> and the <sup>13</sup>C chemical shift was referenced to the -CH<sub>2</sub>- signal of the EO moieties of the PEO-PPO-PEO triblock copolymer, which was assigned a chemical shift of 71 ppm.<sup>61</sup>

**NMR Cross-Relaxation Measurements.** NMR-active nuclei in close spatial proximities tend, in the absence of fast isotropic motions, to exhibit significant dipole-dipole-coupling-induced cross-relaxation due to the nuclear Overhauser effect (NOE). The strength of cross-relaxation interactions scales as  $r^{-6}$ , where  $r$  is the distance separating two dipole-dipole-coupled nuclei, so that such measurements can sensitively probe molecular proximities. Here, rotating-frame nuclear Overhauser effect (ROE) <sup>1</sup>H NMR spectra were acquired by using a selectively excited gradient-selected pulse sequence<sup>62</sup> with a continuous wave spin-lock field strength of approximately 3500 Hz. ROE measurements were carried out because of the dependence of the signs of the NOE cross-relaxation peaks on the associated molecular rotational correlation time. For short rotational correlation times, positive NOE cross-relaxation peaks are typically observed, while

(53) Zhang, Y. H.; Guo, L.; Ma, C.; Li, Q. S. *Phys. Chem. Chem. Phys.* **2001**, *3*, 583–587.

(54) Lebens, P. J. M.; Keurentjes, J. T. F. *Ind. Eng. Chem. Res.* **1996**, *35*, 3415–3421.

(55) Momot, K. I.; Kuchel, P. W.; Chapman, B. E.; Deo, P.; Whittaker, D. *Langmuir* **2003**, *19*, 2088–2095.

(56) Vuister, G. W.; Boelens, R.; Kaptein, R.; Hurd, R. E.; John, B.; Vanzijl, P. C. M. *J. Am. Chem. Soc.* **1991**, *113*, 9688–9690.

(57) Willker, W.; Leibfritz, D.; Kerssebaum, R.; Bermel, W. *Magn. Reson. Chem.* **1993**, *31*, 287–292.

(58) Shaka, A. J.; Barker, P. B.; Freeman, R. *J. Magn. Reson.* **1985**, *64*, 547–552.

(59) Hand, E. S.; Cohen, T. *J. Am. Chem. Soc.* **1965**, *87*, 133–134.

(60) Gottlieb, H. E.; Kotlyar, V.; Nudelman, A. *J. Org. Chem.* **1997**, *62*, 7512–7515.

(61) Melosh, N., Ph.D. Thesis, Department of Materials, University of California, Santa Barbara, 2002.

(62) Dalvit, C.; Bovermann, G. *Magn. Reson. Chem.* **1995**, *33*, 156–159.



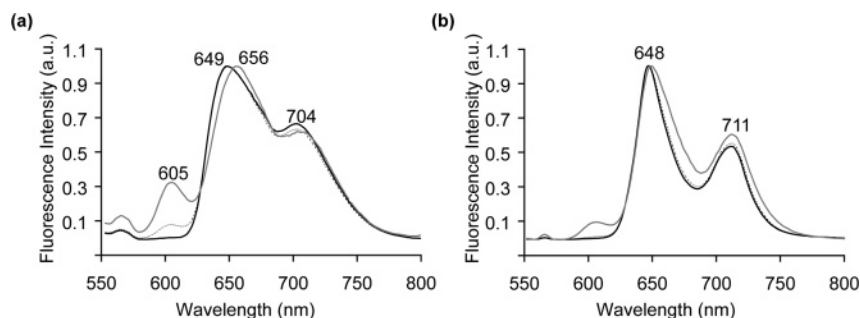


**Figure 2.** Fluorescence spectra of 10 mM tetra(4-sulfonatophenyl)porphyrin (TPPS<sub>4</sub>) in aqueous solutions (pH = 11) in (a) the absence and (b) the presence of 10 mM EO<sub>20</sub>-PO<sub>70</sub>-EO<sub>20</sub> (P123) triblock copolymer species. Spectra were obtained at 15 °C (solid black line), 23 °C (dotted black line), and 40 °C (solid gray line).

this problem significantly by resolving the signals and decays associated with the individual components and also allows the resulting diffusivities to be assigned unambiguously to the species associated with various resonances. All diffusion coefficients were normalized to that of HDO in D<sub>2</sub>O. To verify the effectiveness of the convection-compensating double stimulated-echo technique over the range of temperatures used, the measured HDO diffusion coefficients were compared to previously published<sup>77</sup> viscosity data for D<sub>2</sub>O using the Stokes–Einstein equation, with excellent agreement observed.

**NMR Measurements of Molecular Exchange Dynamics.** Molecular exchange dynamics between solution and micelle species were probed by performing 1D PG-DSTE <sup>1</sup>H NMR measurements over a range of diffusion times. For diffusion times that are short with respect to the exchange time between two states, an observed signal decay will reflect a superposition of the two decays associated with the two states. By increasing the diffusion time to values that are large compared to the exchange time, the relative importance of the faster-diffusing component increases. This is because the magnetization associated with the fast-diffusing component dephases more quickly, with the result that this state acts as an exchange sink from which magnetization cannot be recovered. The time scales of exchange processes that can be studied with this technique are limited by the diffusion time necessary to obtain adequate signal attenuation to establish the multiexponential character of the diffusion process. For a maximum available gradient strength of 6.65 G/mm, it is possible to investigate exchange times on the order of 100 ms when large micellar aggregates are involved.

By assuming a two-site process for the exchange of TPPS<sub>4</sub> dye species between PEO–PPO–PEO unimers and micelle environments, TPPS<sub>4</sub> residence times in each of the two states were determined by a global nonlinear least-squares fit (using the Levenberg–Marquand algorithm<sup>78</sup>) of the experimental data to governing equations derived by Kärger.<sup>79,80</sup> The stability of the fitting results with respect to experimental uncertainty in the data was investigated by carrying out a Monte Carlo-type error analysis. Alper and Gelb have described this approach in detail and showed that such an analysis results in more-reliable error estimates for systems with strongly covariant fitting parameters, such as the one considered here.<sup>81</sup> To avoid complications resulting from potentially different *T*<sub>1</sub> relaxation times for the various species present in solution, an additional delay was introduced into the standard pulse sequence, so that the sums of the eddy-current delays and the diffusion times were kept constant. As the magnetization was stored along the *z* axis during both delays, this modification compensated for *T*<sub>1</sub>-relaxation effects that otherwise could arise from the use of different experiment times. This modification, however, does not strictly remove the possibility that concurrent diffusion and relaxation processes could both contribute to signal attenuation during the

variable diffusion delay time. Because it is not possible to separate the signal decays that arise from independent spin-relaxation and diffusion effects, it is typically necessary to fit the data to a model that is based not only on relative species populations (i.e., residence times) and diffusion coefficients in the different environments but also on their respective *T*<sub>1</sub> relaxation times. Here, however, only a single *T*<sub>1</sub> relaxation time was observed in separate inversion–recovery experiments for the TPPS<sub>4</sub> resonance investigated, specifically *T*<sub>1</sub> = 2.4 s for the phenyl protons in ortho positions with respect to the central macrocycle. Moreover, this *T*<sub>1</sub> value is significantly larger than the maximum diffusion time used in the experiments ( $\Delta = 500$  ms), so that relaxation contributions which might otherwise skew the relative species populations are expected to be negligible.

**Differential Scanning Calorimetry.** Differential scanning calorimetry (DSC) was used to examine the bulk micellization behavior of PEO–PPO-based triblock copolymers in solution. In general, DSC can provide the temperature at which micellization in solution begins and the range of temperatures over which it occurs. It is furthermore possible to quantify the change in free energy associated with micellization. DSC measurements were performed on the same samples as used in the NMR investigations described above using a TA Instruments calorimeter. The temperature of the sample compartment was lowered to 5 °C before insertion of each separately sealed and refrigerated (~5 °C) sample pan. Each sample was then allowed to equilibrate for 20 min before scanning. After reaching the final temperature of 60 °C, each sample was cooled to 5 °C and the measurement repeated to ensure reproducibility.

**Fluorescence Spectroscopy.** Fluorescence spectroscopy is sensitive to the molecular environments of a fluorophore that are the primary bases for observed Stokes shifts. In many cases, it is thus possible to infer the location of dye species on the basis of the observed changes in the fluorescence spectrum. Temperature-dependent fluorescence measurements were conducted in sealed capillary tubes on a Varian Cary Eclipse fluorimeter with a Peltier-controlled constant-temperature water bath. The samples were allowed to equilibrate at the desired temperature for at least 20 min before each measurement.

## Results and Discussion

### Localization of Guest–Host Interaction Sites.

**Evidence for TPPS<sub>4</sub>–P123 Interactions: Fluorescence Measurements.** Fluorescence spectra shown in Figure 2 for TPPS<sub>4</sub> dissolved in water and in aqueous EO<sub>20</sub>-PO<sub>70</sub>-EO<sub>20</sub> triblock copolymer (P123) solutions reveal evidence of interactions of the P123 triblock copolymer with the dissolved dye species. For alkaline aqueous solutions (pH = 11) of 10 mM TPPS<sub>4</sub> at 15 °C, two main bands are observed (Figure 2a), corresponding to a (0–0) transition at 649 nm and its vibronic (0–1) transition at 704 nm. Upon addition of 10 mM P123, the vibronic transition appears at 711 nm and both transitions are more sharply defined (Figure 2b). The changes in line widths and position indicate that the TPPS<sub>4</sub> dye species interact with the triblock copolymer in solution, although the nature of this interaction is not clear. No significant changes in the

(77) Cho, C. H.; Urquidí, J.; Singh, S.; Robinson, G. W. *J. Phys. Chem. B* **1999**, *103*, 1991–1994.

(78) Press, W. H.; Teukolsky, S. A.; Vetterling, W. T.; Flannery, B. P., Eds. *Numerical Recipes in C++: The Art of Scientific Computing*, 2nd ed.; Cambridge University Press: Cambridge, 2002.

(79) Kärger, J. *Ann. Phys.* **1969**, *7*, 1–4.

(80) Kärger, J. *Ann. Phys.* **1971**, *7*, 107–109.

(81) Alper, J. S.; Gelb, R. I. *J. Phys. Chem.* **1990**, *94*, 4747–4751.

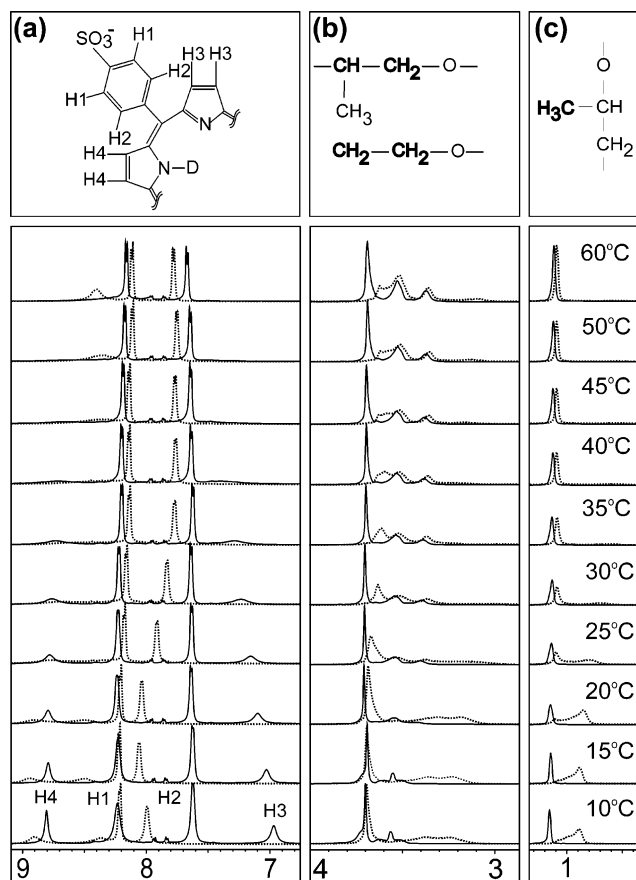


**Figure 3.** One-dimensional  $^1\text{H}$  NMR spectra showing (a) the aromatic region of a 10 mM aqueous solution (pH = 11) of tetra-(4-sulfonatophenyl)porphyrin (TPPS<sub>4</sub>) in the absence (solid lines) and presence (dotted lines) of 10 mM P123 block copolymer; (b) the  $-\text{CH}-$ ,  $-\text{CH}_2-$ , and (c)  $-\text{CH}_3$  spectral regions of a 10 mM aqueous solution (pH = 11) of P123 in the absence (solid lines) and in the presence (broken lines) of 10 mM TPPS<sub>4</sub>. Spectra were collected over a range of temperatures from 10 to 60 °C. Significant spectral changes were observed with increasing temperature for all resonances. The proton moieties giving rise to the signals in parts (a), (b), and (c) are indicated in the boxes above each set of spectra, respectively.

two bands are observed for either solution upon increasing the temperature from 15 to 23 °C, but a further increase to 40 °C leads to a small red shift ( $\sim 1$ –2 nm) of both bands and the appearance of a third band at approximately 605 nm. From these measurements alone, it is not possible to draw detailed conclusions about structural or dynamic interactions between the dye and triblock copolymer species at a molecular level.

**Assignment of NMR Signals in Separate P123 and TPPS<sub>4</sub> Solutions.** In comparison, NMR spectroscopy yields detailed insights on the molecular environments and aggregation behaviors of both the dye and the triblock copolymer species and, more importantly, provides the opportunity to correlate these data. Before investigating the interactions between the dye and triblock copolymer species in solution, spectroscopic analyses and assignments of the observed  $^1\text{H}$  NMR resonances were first carried out for separate aqueous solutions (pH = 11) of TPPS<sub>4</sub> and P123 over the temperature range 10–60 °C. The corresponding solution-state  $^1\text{H}$  NMR spectra of these separate aqueous solutions are shown as solid lines in Figure 3. The TPPS<sub>4</sub> dye species dissolved in D<sub>2</sub>O (Figure 3a, solid lines) gives rise to four resolved signals in the aromatic region of the  $^1\text{H}$  spectrum (between 7 and 9 ppm), which were assigned according to previous work by Corsini

and Herrmann.<sup>44</sup> Specifically, the intense resonance observed at 7.6 ppm (H2) at all temperatures investigated was assigned to the eight equivalent protons in the ortho positions of the four phenyl rings with respect to the central macrocycle. The second resonance of the same integrated intensity, observed at 8.2 ppm (H1) for all temperatures investigated, was similarly assigned to the eight equivalent protons in meta positions of the four phenyl rings. The less-intense resonances at 8.8 and 7.0 ppm observed at 10 °C correspond to the remaining protons directly bound to the central macrocycle: the resonance at 8.8 ppm (H4) was assigned to the four equivalent protons of the two pyrrole rings that are deuterated at the nitrogen sites and that at 7.0 ppm (H3) to the four protons of the two pyrrole rings with nitrogen atoms not bound to deuterons in alkaline D<sub>2</sub>O solutions. As the temperature is increased, the positions and relative intensities of the two intense resonances, H1 and H2, do not change significantly, while the remaining two resonances, H3 and H4, are broadened and their chemical shift difference decreases. This is a reflection of the increasing rate of tautomerization of the deuterons bound to the pyrrole nitrogen atoms of the central porphyrin macrocycle.<sup>82,83</sup>

Overlap of the  $^1\text{H}$  resonances associated with the similar PEO and PPO moieties in an aqueous solution (pH = 11) of 10 mM P123 made direct assignments of most of the resonances from the 1D  $^1\text{H}$  NMR spectra alone impossible. The proton resonance at 1.2 ppm was assigned to the  $-\text{CH}_3$  methyl groups of the PPO blocks, but it was not possible to assign the remaining  $-\text{CH}_2-$ / $-\text{CH}-$  resonances. To overcome the resolution limitations of the 1D  $^1\text{H}$  spectra, two-dimensional (2D) HSQC  $^1\text{H}\{^{13}\text{C}\}$  NMR spectra were acquired to spread and correlate frequencies in a 2D map. This permitted all  $^{13}\text{C}$  and  $^1\text{H}$  resonances to be resolved and assigned. The  $-\text{CH}_2-$ / $-\text{CH}-$  regions of HSQC  $^1\text{H}\{^{13}\text{C}\}$  NMR spectra acquired at different temperatures are shown in Figure 4 as gray lines. Assignments of these moieties were further aided by the use of gradient-selected multiplicity-edited HSQC experiments in which the sign of spectral intensity of an observed resonance depends on the number of protons bonded to a particular carbon site.<sup>57</sup> This allowed the assignment of the signal with a  $^1\text{H}$  chemical shift of 3.7 ppm and a  $^{13}\text{C}$  chemical shift of 77 ppm to the  $-\text{CH}-$  moieties of the PPO blocks. The more-intense of the remaining  $-\text{CH}_2-$  resonances with a  $^1\text{H}$  chemical shift of 3.6 ppm and a  $^{13}\text{C}$  chemical shift of 71 ppm was assigned to the  $-\text{CH}_2-$  groups of the PEO blocks, because there are approximately 80 PEO  $-\text{CH}_2-$  groups versus 70 PPO  $-\text{CH}_2-$  groups in each P123 triblock copolymer molecule. The remaining peak, with a  $^1\text{H}$  chemical shift of approximately 3.5 ppm and a  $^{13}\text{C}$  chemical shift of about 73 ppm, was assigned to the PPO  $-\text{CH}_2-$  moieties. With increasing temperature, the shape and position of the peak associated with the PEO  $-\text{CH}_2-$  moieties remains essentially constant, while the signals associated with the PPO moieties show small changes that are consistent with the expulsion of water from the PPO blocks with increasing temperature. The identities of all of the observed  $^1\text{H}$  and  $^{13}\text{C}$  resonances in separate aqueous solutions of TPPS<sub>4</sub> and P123 triblock copolymer species are thus established under alkaline solution conditions (10 mM concentrations, pH = 11).

**Evidence of TPPS<sub>4</sub>–P123 Interactions:  $^1\text{H}$  NMR.** Comparing the separate TPPS<sub>4</sub> and P123 solutions with an aqueous mixture of both species under otherwise identical

(82) Storm, C. B.; Teklu, Y. *J. Am. Chem. Soc.* **1972**, *94*, 1745–1747.

(83) Schlabach, M.; Wehrle, B.; Rumpel, H.; Braun, J.; Scherer, G.; Limbach, H. H. *Ber. Bunsen. Ges. Phys. Chem.* **1992**, *96*, 821–833.

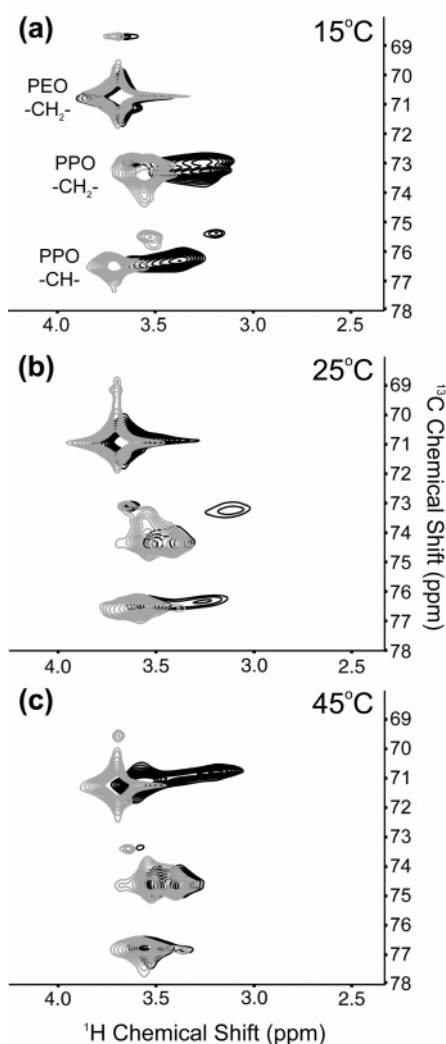


**Figure 4.** Two-dimensional heteronuclear single-quantum-coherence (HSQC)-resolved  $^1\text{H}\{^{13}\text{C}\}$  NMR spectra of the  $-\text{CH}_2-$  and  $-\text{CH}-$  region (2.5–4 ppm) acquired for a 10 mM aqueous solution (pH = 11) of  $\text{EO}_{20}-\text{PO}_{70}-\text{EO}_{20}$  (P123) block copolymer species in the absence (gray) and in the presence (black) of 10 mM tetra(4-sulfonatophenyl)porphyrin (TPPS<sub>4</sub>). Spectra recorded at (a) 15, (b) 25, and (c) 45 °C show differences in the PPO region (resonances with  $^{13}\text{C}$  chemical shifts above 72 ppm) at the two lower temperatures, while at 45 °C, spectral differences are observed only for the PEO resonance ( $^{13}\text{C}$  chemical shift of approximately 71 ppm).

conditions reveals noticeable differences in the positions and line widths of signals in the  $^1\text{H}$  NMR spectra. Such differences can be analyzed in detail to determine the loci of interactions between the different species in solution. When two moieties are in close spatial proximity, the local electronic environments of either or both species may be perturbed, altering the local magnetic fields experienced by their nuclei and leading to changes in their observed isotropic chemical shifts. Provided that they are not averaged by rapid isotropic molecular motions,<sup>84–86</sup> these perturbations can be especially prominent for aromatic molecules (such as TPPS<sub>4</sub>) in which the highly mobile  $\pi$ -electrons give rise to ring currents in the presence of magnetic fields.<sup>87,88</sup> Such chemical-shift perturbations induced by interactions among molecular species are observed in the single-pulse  $^1\text{H}$  NMR spectra (Figure 3,

dotted lines) for both the TPPS<sub>4</sub> dye and the P123 triblock copolymer species in their aqueous mixture. Comparison with the  $^1\text{H}$  NMR spectra acquired from separate aqueous solutions of TPPS<sub>4</sub> (Figure 3a, solid lines) and P123 (Figure 3b and c, solid lines) reveal significant differences in the isotropic chemical shifts of numerous moieties. These differences establish that the two species experience strong mutual interactions in solution over the range of temperatures (10–60 °C) examined. For example, at 10 °C, the resonances associated with the H2 and H3 protons of the dye experience significant increases in their chemical shift values from 7.6 to 8.0 ppm and from 7.0 to 8.4 ppm, respectively (based on separate  $^1\text{H}\{^{13}\text{C}\}$  HSQC measurements not shown here). At the same temperature, the triblock copolymer species are also significantly affected by interactions with the dye molecules, as reflected by the shift and broadening of the signal associated with the methyl protons of the PPO blocks from 1.2 to 0.9 ppm. The spectral changes are not limited to these resonances, however, and the underlying interactions are noticeably influenced by temperature.

*Effects of TPPS<sub>4</sub>–P123 Interactions on TPPS<sub>4</sub>: Changes in  $^1\text{H}$  NMR Spectra.* The changes in the aromatic region (7–9 ppm) of the  $^1\text{H}$  spectrum upon mixing of the P123 triblock copolymer and TPPS<sub>4</sub> dye species reflect the effect of the polymer on the dye. In contrast to the H2 protons mentioned above, the chemical shift of the H1 protons of the TPPS<sub>4</sub> species decreases slightly (<0.1 ppm at 10 °C) as a result of their interaction with the P123 species. As the temperature is increased, the magnitude of this chemical shift change increases, reaching a maximum of 0.1 ppm (8.1 versus 8.0 ppm) at temperatures above 25 °C. The chemical shift of the H2 protons shows a more pronounced temperature dependence. As the temperature is increased, the chemical shift increases between 0.1 and 0.5 ppm with respect to its value at 10 °C, reaching a maximum at 15 °C and then diminishing until becoming constant at approximately 7.7 ppm above 45 °C. This difference in behavior may be due to interactions of the undeuterated nitrogen atoms of the central TPPS<sub>4</sub> macrocycle with the triblock copolymer species: an increase in the electron-withdrawing character of the central macrocycle with respect to the peripheral phenyl rings due to interactions with the P123 species would produce the observed chemical shift effects, i.e., a deshielding of the H2 protons in the ortho position.

The composition- and temperature-dependent changes in the H1 and H2 chemical shifts are consistent with those observed for the H3 and H4 resonances associated with the TPPS<sub>4</sub> pyrrole rings with and without deuterated nitrogen moieties, respectively. At 10 °C, the signal corresponding to the H3 protons moves significantly downfield and is broadened as a result of interactions with the triblock copolymer species, exhibiting an increase

(86) Establishing whether ring-current-induced changes in chemical shifts occur when different species interact in solution is complicated by the fact that such interactions depend both on the distance between the two moieties and on their relative reorientation dynamics. Rapid reorientation of the two moieties with respect to each other tends to average the effective perturbation with respect to the static external magnetic field. This means that two spatially proximate molecules experiencing independent isotropic motions will generally not show ring-current induced differences in their chemical shifts, while two spatially close moieties with fixed relative orientations may experience very large chemical-shift influences. The presence of such a chemical-shift effect therefore implies close spatial proximity, although the absence of such a shift does not, in general, rule this out due to the strong covariance that may exist between distance and relative dynamics.

(87) Pauling, L. J. *Chem. Phys.* **1936**, *4*, 673–677.

(88) Becker, E. D.; Bradley, R. B. *J. Chem. Phys.* **1959**, *31*, 1413–1414.

(84) Stilbs, P. J. *Colloid Interface Sci.* **1983**, *94*, 463–469.

(85) Eriksson, J. C.; Gillberg, G. *Acta Chem. Scand.* **1966**, *20*, 2019–2027.

of 1.4 ppm in chemical shift to 8.4 ppm, thus indicating substantial deshielding. On the other hand, the signal corresponding to the H4 protons, which are directly associated with the pyrrole rings containing the deuterated nitrogen sites, does not show pronounced chemical shift changes. The temperature dependences of the H3 and H4 proton resonances of the TPPS<sub>4</sub> molecules in the presence or absence of the triblock copolymer species are similar: as the temperature is increased, the corresponding proton signals become broadened and their relative chemical shift differences decrease, likely as a result of an increasing rate of tautomerization of the deuterons bound to the pyrrole nitrogen sites. At temperatures above 45 °C, the H3 and H4 resonances observed for the aqueous TPPS<sub>4</sub>/P123 mixture coalesce into a single peak. Previous studies<sup>44</sup> have shown that this effect does not occur in aqueous TPPS<sub>4</sub> solutions until above approximately 90 °C, indicating that interactions with the P123 triblock copolymer species promote an increased rate of exchange of the central TPPS<sub>4</sub> deuterons.<sup>89</sup>

<sup>1</sup>H NMR spectra of P123 and TPPS<sub>4</sub> in acidic solutions (pH = 1), in which all four nitrogen sites of the TPPS<sub>4</sub> dye species are deuterated, were obtained to investigate the roles of these central macrocycle sites in promoting interactions with the block copolymer species. In this case, the proposed interaction sites (i.e., the undeuterated nitrogen moieties) of the porphyrin species are effectively blocked by deuterium atoms and, indeed, no chemical shift changes are observed for any of the P123 <sup>1</sup>H NMR signals upon mixing with the acid form of the TPPS<sub>4</sub> dye. These results indicate that the undeuterated pyrrole nitrogen moieties are the primary interaction sites between the TPPS<sub>4</sub> dye and P123 triblock copolymer species in aqueous solution.

*Effects of TPPS<sub>4</sub>-P123 Interactions on P123: Changes in <sup>1</sup>H and <sup>1</sup>H{<sup>13</sup>C} Spectra.* After mixing the TPPS<sub>4</sub> dye and the P123 triblock copolymer species in solution, their interactions also produce significant temperature-dependent changes in the regions of the <sup>1</sup>H NMR spectrum corresponding to the triblock copolymer moieties (0–2 and 3–4 ppm). Similar to the methyl groups of the PPO block discussed above, the <sup>1</sup>H signals associated with the remaining PEO and PPO moieties of the P123 triblock copolymer show significant chemical-shift changes that are strongly influenced by temperature, similar to those observed in the aromatic region for the TPPS<sub>4</sub> dye species (<sup>1</sup>H chemical shifts between 7 and 9 ppm). At 10 °C, the signal associated with the methyl groups of the PPO block (Figure 3c) shows significant inhomogeneous broadening, with a maximum intensity at 0.90 ppm, corresponding to an upfield shift of approximately 0.25 ppm, compared to the D<sub>2</sub>O/P123 solution without TPPS<sub>4</sub>. As the temperature is increased, the low-field portion of this signal (1.0–1.1 ppm) grows at the expense of the high-field portion (0.8–1.0 ppm) until the high-field resonance disappears completely near 35 °C. As discussed in more detail below, the high-field signal corresponds to –CH<sub>3</sub> groups of the PPO block that interact with and are affected by the presence of the TPPS<sub>4</sub> dye species. The low-field signal has essentially the same chemical shift as the –CH<sub>3</sub> moieties in a D<sub>2</sub>O/P123 triblock copolymer solution and, thus, is attributed to a fraction of the PPO methyl groups that do not experience strong interactions with the dye species. This suggests that the TPPS<sub>4</sub> species interact strongly

with the PPO blocks in solution at low temperatures and that the importance of this interaction decreases with increasing temperature.

The remaining resonances observed in the 1D <sup>1</sup>H spectra of Figure 3b for the TPPS<sub>4</sub>- and P123-containing solutions correspond to the –CH<sub>2</sub>– and –CH– groups of the PPO blocks and the –CH<sub>2</sub>– groups of the PEO blocks, all of which overlap. These signals are resolved in the 2D <sup>1</sup>H-<sup>13</sup>C} HSQC spectra shown in Figure 4 acquired at 15, 25, and 45 °C, where the gray and black contour lines correspond to aqueous P123 solutions without and with TPPS<sub>4</sub>, respectively. <sup>13</sup>C and <sup>1</sup>H chemical shift correlations are clearly observed between different *J*-coupled nuclei, which allow the resonances from these similar moieties to be assigned unambiguously. The signals associated with the –CH<sub>2</sub>– (<sup>13</sup>C chemical shift of 73 ppm) and –CH– (<sup>13</sup>C chemical shift of 76 ppm) moieties of the PPO blocks show the same qualitative behaviors as observed for the –CH<sub>3</sub> PPO groups: at low temperatures (15 °C, Figure 4a) the peaks are inhomogeneously broadened in the <sup>1</sup>H dimension and appear at ~0.3 ppm lower <sup>1</sup>H chemical shift values, compared to the aqueous P123 solution. As the temperature is increased (25 °C, Figure 4b), the portion of the inhomogeneously broadened signal observed at lower chemical shift values in the <sup>1</sup>H dimension diminishes and disappears completely at higher temperatures (45 °C, Figure 4c). This is consistent with strong interactions of the PPO blocks with the TPPS<sub>4</sub> guest species at low temperatures (15 °C) and diminished interactions at higher temperatures (>25 °C).

The signal associated with the –CH<sub>2</sub>– moieties of the PEO block (<sup>13</sup>C chemical shift of 71 ppm) shows the opposite trend. At low temperatures (15 °C, Figure 4a), no differences in the <sup>1</sup>H chemical shift or inhomogeneous broadening in the <sup>1</sup>H dimension were observed before and after mixing with TPPS<sub>4</sub>. As the temperature is increased, however, the corresponding signal becomes inhomogeneously broadened and at 45 °C (Figure 4c) a significant shoulder at lower <sup>1</sup>H chemical shift values (3.0–3.5 ppm) is observed, with a chemical shift difference of approximately 0.5 ppm compared with the aqueous P123 solution. The observed changes in the positions and line shapes of signals in the 1D <sup>1</sup>H NMR spectra (Figure 3b, c) and the correlated 2D <sup>1</sup>H{<sup>13</sup>C} NMR spectra (Figure 4) thus clearly establish that the locus of preferred interaction with the TPPS<sub>4</sub> dye species with the various PEO and PPO triblock copolymer moieties is highly temperature dependent.

The gradual and monotonic nature of the observed changes in <sup>1</sup>H chemical shifts with increasing temperature is consistent with the increasing relative hydrophobicity of the propylene oxide moieties of the P123 triblock copolymer in solution. At low temperatures (<20 °C), the TPPS<sub>4</sub> dye species interact preferentially with the PPO blocks. As the temperature is increased, however, TPPS<sub>4</sub> interactions with the more hydrophilic PEO blocks become favored until, at temperatures above 35 °C, the TPPS<sub>4</sub> species interact exclusively (within the resolution limits of the NMR measurements) with the PEO blocks. Thus, a slow physical crossover of the TPPS<sub>4</sub> species from the PPO blocks of the P123 triblock copolymer to the PEO block occurs with increasing temperature.

*Effects of TPPS<sub>4</sub>-P123 Interactions: <sup>1</sup>H Cross-Relaxation Measurements.* ROE measurements confirm the different temperature-dependent interactions between the TPPS<sub>4</sub> guest species and the different moieties of the P123 host. Proton cross-relaxation by the NOE<sup>63</sup> is mediated by through-space dipole–dipole couplings, which can be used to probe molecular proximity. Intermolecular <sup>1</sup>H

(89) In principle, it is possible to derive an activation energy for the tautomerization process from the temperature dependence of the splitting between the corresponding signals. However, for this system, the local environments experienced by the porphyrin molecules also change with temperature, which complicates the analysis.



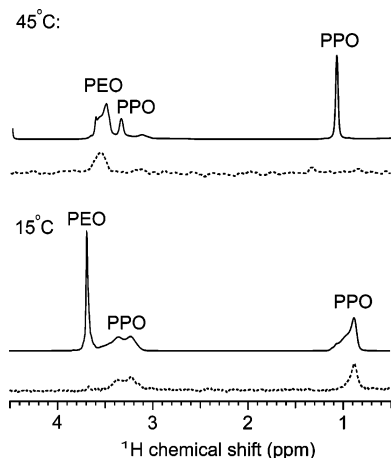


**Figure 5.** One-dimensional rotating-frame nuclear Overhauser effect (ROE)  $^1\text{H}$  NMR spectra (broken lines) of an aqueous solution (pH = 11) of 10 mM tetra(4-sulfonatophenyl) porphyrin (TPPS<sub>4</sub>) and 10 mM EO<sub>20</sub>-PO<sub>70</sub>-EO<sub>20</sub> (P123) block copolymer species. Spectra were recorded at 15 and 45 °C by selectively exciting the phenyl protons in the ortho position with respect to the central macrocycle of the TPPS<sub>4</sub> dye species and observing the appearance of cross-relaxation peaks in the spectral region corresponding to the triblock copolymer species. Conventional single-pulse 1D  $^1\text{H}$  NMR spectra (solid lines) are shown for comparison.

cross-relaxation processes can, in general, occur for molecules that are in close spatial contact (on the order of 0.1–1 nm). In a typical experiment, the  $^1\text{H}$  resonance of a certain moiety is excited selectively and cross-relaxation processes to other proton moieties are monitored. In this case, the TPPS<sub>4</sub> phenyl protons in the ortho positions (H2) relative to the central macrocycle were selectively excited to take advantage of their strong signal intensity and their close spatial proximities to the principal porphyrin interaction sites at the undeuterated pyrrole nitrogen atoms. Figure 5 shows the  $^1\text{H}$  cross-relaxation ROE spectra (dotted lines) and standard 1D  $^1\text{H}$  NMR spectra (solid lines) for the spectral region 0.5–4.5 ppm, corresponding to the  $-\text{CH}_2-$ ,  $-\text{CH}-$ , and  $-\text{CH}_3$  moieties of the P123 triblock copolymer in aqueous alkaline P123/TPPS<sub>4</sub> solution. At 15 °C, proton cross-relaxation peaks are observed at chemical shifts corresponding to  $^1\text{H}$  signals only associated with the PPO blocks of the P123 species (0.9 and 3.2–3.4 ppm). At 45 °C, these cross-relaxation peaks are not observed, but a new cross-relaxation peak at 3.5 ppm is present, which corresponds to the  $-\text{CH}_2-$  moieties of the PEO blocks. These proton cross-relaxation ROE results thus confirm the strong interactions of the TPPS<sub>4</sub> dye molecules with the PPO blocks at low temperatures (<20 °C) and that the locus of interaction changes to the PEO blocks with increasing temperature.

**Triblock Copolymer Micellization in the Presence of TPPS<sub>4</sub>.** *Effect of TPPS<sub>4</sub> on P123 Micellization: Calorimetric Measurements.* While the TPPS<sub>4</sub> dye molecules have been shown above to associate selectively with different PEO and PPO moieties depending on the solution conditions, whether and to what extent the guest species may perturb the self-assembly behavior of the triblock copolymer species is challenging to establish. It is reasonable to expect that the strong guest–host interactions observed may influence the micellization behavior of the system, that is, whether the P123 triblock copolymer species are self-assembled into micelles or whether a significant fraction persists in solution as unimers or as small aggregates. Micellization in aqueous solutions of amphiphilic triblock copolymers can be studied in a

number of ways,<sup>90</sup> including surface tension measurements, light scattering, DSC, and the measurement of diffusion coefficients using pulsed-gradient NMR spectroscopy. As the presence of significant amounts of strongly light-absorbing dye species in the aqueous TPPS<sub>4</sub>/P123 mixture resulted in optically dense solutions, DSC measurements were preferred over light-scattering studies, which can be challenging to conduct and interpret for such systems. DSC traces were acquired for a solution of 10 mM P123 in D<sub>2</sub>O at pH 11, both in the absence and in the presence of 10 mM TPPS<sub>4</sub>. Notably, it was found by DSC that the CMT (corresponding to the temperature at which the maximum energy is absorbed upon heating the solution, which corresponds to the maximum rate of micelle formation) changes from 15 to 20 °C in the presence of the TPPS<sub>4</sub> guest species. This change in the micellization temperature suggests that strong interactions between the P123 triblock copolymer species and the TPPS<sub>4</sub> dye molecules stabilize small TPPS<sub>4</sub>-P123 complexes. The DSC measurements, however, provide little molecular-level information about the micellization process.

*Diffusion Behavior of TPPS<sub>4</sub> and P123 in Separate Solutions: PG-DSTE  $^1\text{H}$  NMR.* Pulsed-gradient  $^1\text{H}$  NMR techniques, on the other hand, in combination with 2D  $^1\text{H}\{^{13}\text{C}\}$  HSQC methods, provide unambiguous evidence of the molecular origins of the dye–triblock copolymer interactions and the resulting micellization behavior. Such measurements can be used to determine the self-diffusion coefficients of all spectroscopically distinct species in a solution. These self-diffusion coefficients can further be related to an effective size of the diffusing species through the Stokes–Einstein relation ( $D \propto 1/r$ , where  $D$  is the self-diffusion coefficient and  $r$  is the effective radius of the species).<sup>91</sup> It is thus possible, for example, to distinguish micelles from P123 unimers, as well as TPPS<sub>4</sub> dye molecules associated with these species. The dotted lines in Figure 6 correspond to self-diffusivities of TPPS<sub>4</sub> and P123 species that have been normalized with respect to the diffusivity of water, as measured by PG-DSTE  $^1\text{H}$  NMR in separate aqueous (pH = 11) 10 mM solutions; the solid lines correspond to their relative diffusivities in an aqueous solution containing 10 mM of both TPPS<sub>4</sub> and P123. In addition, a second vertical axis is included on the right, showing the corresponding size estimates based on the Stokes–Einstein relationship. The relative diffusion coefficient of the TPPS<sub>4</sub> dye species (measurements for the H1 and H2 resonances gave equivalent results) in D<sub>2</sub>O remains essentially constant at  $D_{\text{TPPS}_4}/D_{\text{water}} = 0.086$  as the temperature is varied from 10 to 60 °C under alkaline solution conditions, suggesting that little aggregation or deaggregation of TPPS<sub>4</sub> occurs with increasing temperature. These results are consistent with the absence of significant changes in the fluorescence spectra over this temperature range.

In comparison, the measured diffusion coefficient of the P123 triblock copolymer species (measurements for the  $-\text{CH}_2-$ ,  $-\text{CH}-$ , and  $-\text{CH}_3$   $^1\text{H}$  resonances yielded equivalent results) in D<sub>2</sub>O decreases by approximately a factor of 3.3 from  $D_{\text{P123}}/D_{\text{water}} = 0.026$  to 0.008 as the temperature increased from approximately 15 to 30 °C. The reported values are average diffusion coefficients, reflecting both fast-diffusing unimers in solution and slow-diffusing micellar aggregates. Because exchange between the two populations is fast compared to the diffusion times used in these measurements,<sup>92</sup> a single-exponential decay was

(90) Booth, C.; Attwood, D. *Macromol. Rapid Comm.* **2000**, *21*, 501–527.

(91) Stachel, J., Ed. *The Collected Papers of Albert Einstein*; Princeton University Press: Princeton, NJ, 1989; Vol. 2.

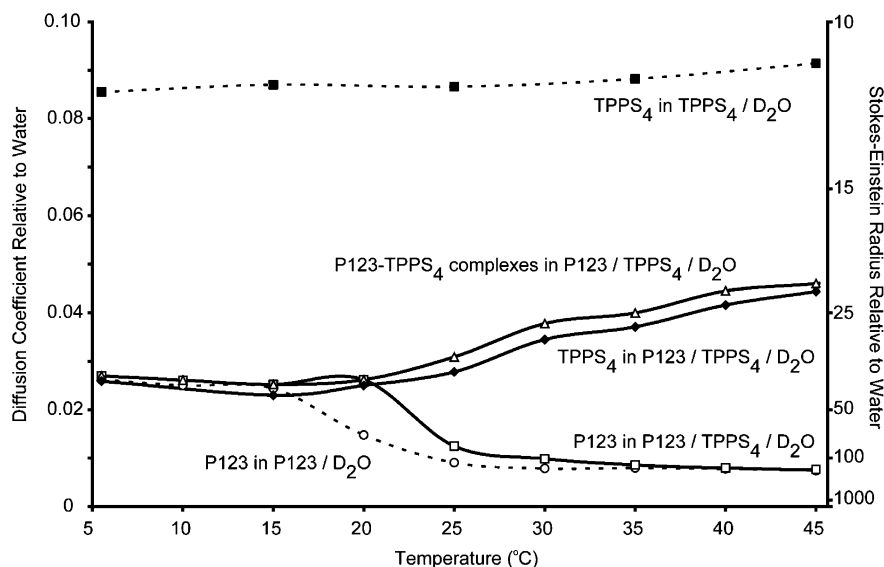


**Figure 6.** Comparison of diffusion coefficients measured by pulsed-gradient double-stimulated-echo (PG-DSTE)  $^1\text{H}$  NMR for the tetra(4-sulfonatophenyl)porphyrin (TPPS<sub>4</sub>) dye (solid black symbols) and the EO<sub>20</sub>-PO<sub>70</sub>-EO<sub>20</sub> (P123) triblock copolymer (hollow symbols) species over the temperature range 5–45 °C. The diffusion coefficients were normalized with respect to the diffusion coefficient of water in D<sub>2</sub>O at each temperature. The diffusion coefficients obtained in aqueous solutions (pH = 11) containing only the TPPS<sub>4</sub> dye species (10 mM) or the P123 triblock copolymer species (10 mM) are indicated by the dotted lines, while those observed in a mixture (10 mM each in TPPS<sub>4</sub> and P123) are indicated by solid lines. The lines are provided to guide the eye.

observed, independent of temperature. Nevertheless, the population of unimers is expected to be very low in binary aqueous P123 solutions at temperatures above the CMT, due to the sharp decrease in the critical micelle concentration with increasing temperature.<sup>6,7</sup> The observed decrease in the diffusivity of P123, corresponding to an estimated increase in volume of the diffusing entity by a factor of approximately 30, is thus consistent with P123 micellization. The onset temperature of this micellization process (~15 °C) is furthermore in good agreement with the calorimetric measurements.

**Diffusion Behavior of TPPS<sub>4</sub>-P123 Mixtures: PG-DSTE  $^1\text{H}$  NMR of TPPS<sub>4</sub> Species.** In an aqueous solution of both 10 mM P123 and TPPS<sub>4</sub>, the TPPS<sub>4</sub> species exhibit significantly lower diffusion coefficients compared to the aqueous TPPS<sub>4</sub> solution. For example, at temperatures below 20 °C, the self-diffusivity of TPPS<sub>4</sub> in the P123-containing solution is  $D_{\text{TPPS}_4}/D_{\text{water}} = 0.027$ , compared with its value of 0.086 in D<sub>2</sub>O. This decrease in the diffusion coefficient is attributed to aggregation of the TPPS<sub>4</sub> species with the P123 triblock copolymer species, which exhibit the same diffusion coefficient at these temperatures, suggesting that the two species are moving as a single complexed entity. There is no evidence of a second component corresponding to a faster-diffusing fraction of uncomplexed TPPS<sub>4</sub> dye molecules. The excellent match of the diffusion coefficients measured for the P123 triblock copolymer moieties and the TPPS<sub>4</sub> dye species suggests that, at these relatively low temperatures (<20 °C), essentially all of the dye molecules are complexed with triblock copolymer species and are interacting preferentially with the PPO blocks. As the temperature is increased above 20 °C, the measured decay curves start to show modest biexponential character, suggesting the presence of two distinct dye populations (see below). The average diffusion coefficients for TPPS<sub>4</sub> increase to approximately  $D_{\text{TPPS}_4}/D_{\text{water}} = 0.044$  at 45 °C, consistent with a decrease in volume of the diffusing entity by approximately a factor of 8. The apparent increase in the diffusivity of TPPS<sub>4</sub>

with temperature could be due to different physical phenomena. One possibility is that a fraction of the TPPS<sub>4</sub> dye molecules desorb from the triblock copolymer species into the aqueous region, where they diffuse in solution as free ions. In this case, the measured diffusion coefficient would represent an average of the freely diffusing fraction of the dye molecules and the fraction of dye molecules that are complexed with the triblock copolymer. Alternatively, some of the TPPS<sub>4</sub> may remain aggregated in small nonmicellar, dye/triblock copolymer complexes that decrease in size as the increasingly hydrophobic PPO chains contract to minimize their exposure to surrounding water, while maintaining strong interactions with the TPPS<sub>4</sub> species. These possibilities can be distinguished experimentally, as described below.

**Diffusion Behavior of TPPS<sub>4</sub>-P123 Mixtures: PG-DSTE  $^1\text{H}$  NMR of P123 Species.** Whether the TPPS<sub>4</sub> species are present as free ions in aqueous solution, complexed with P123 unimers or small aggregates, or included in self-assembled P123 micelles can be determined by comparing the self-diffusion coefficients measured for the TPPS<sub>4</sub> dye molecules with those obtained for the triblock copolymer species. Unfortunately, standard 1D  $^1\text{H}$  PG-DSTE methods lead to the same resolution difficulties for the overlapping polymer resonances as discussed above for Figure 3. However, these resolution challenges can be circumvented by combining 1D  $^1\text{H}$  PG-DSTE and  $^1\text{H}\{^{13}\text{C}\}$  HSQC techniques to resolve and measure the diffusion properties of the different triblock copolymer moieties. In particular, such HSQC-resolved diffusion measurements permit the different PEO and PPO moieties to be distinguished according to whether they are interacting with the dye guests. For example, Figure 7a shows the 2D  $^1\text{H}\{^{13}\text{C}\}$  HSQC spectral region corresponding to the  $-\text{CH}_2-$  moieties of the PEO blocks of the P123 triblock copolymer in an aqueous alkaline 10 mM solution of both P123 and TPPS<sub>4</sub> at 45 °C. Four distinct regions can be identified: Peak 1 exhibits the same  $^{13}\text{C}$  and  $^1\text{H}$  chemical shifts as observed for an aqueous P123 solution in the absence of the dye molecules and is attributed to moieties that are not interacting with the TPPS<sub>4</sub> guest species. The re-

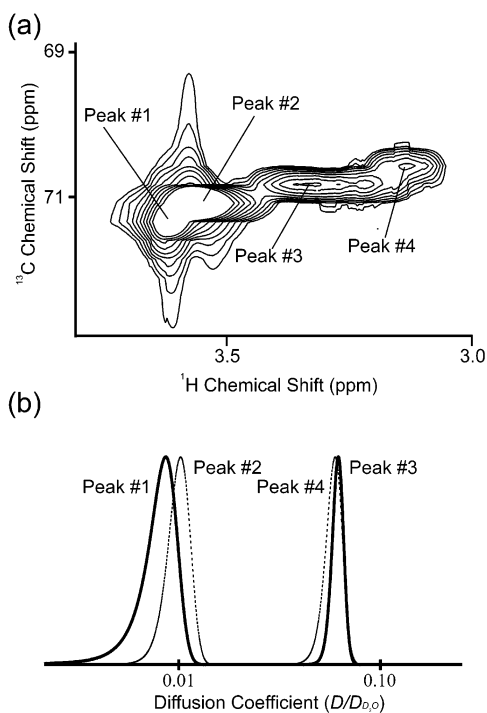


**Figure 7.** Expansion of the region of a diffusion-encoded 2D heteronuclear single-quantum-coherence (HSQC)-resolved  $^1\text{H}\{^{13}\text{C}\}$  NMR spectrum corresponding to the  $-\text{CH}_2-$  moieties of the polyethylene oxide blocks of  $\text{EO}_{20}-\text{PO}_{70}-\text{EO}_{20}$  (P123) triblock copolymer species in an aqueous solution (pH = 11) containing 10 mM tetra(4-sulfonatophenyl)porphyrin (TPPS<sub>4</sub>) and 10 mM P123. The spectrum shown was obtained at 45 °C using 2% of the full gradient strength during diffusion encoding; the experiment was repeated with varying gradient strengths for the determination of diffusion behavior. The corresponding distributions of diffusion coefficients are shown below the spectrum for each of the indicated spectral regions. Two populations are apparent corresponding to P123 micellar aggregates (Peaks 1 and 2) and to P123 unimers or small dye-polymer complexes (Peaks 3 and 4).

maining three peaks, Peaks 2–4, correspond to P123 species interacting with TPPS<sub>4</sub>.

The distribution of diffusion coefficients, reflecting both the range of diffusivities present in the system and the approximate widths of their distributions (see Experimental Section), is shown in Figure 7b. It is clear that the P123 species are present in two very different forms, characterized by self-diffusivities that are an order of magnitude different. Furthermore, on the basis of the DSC results discussed above, the system is well above its CMT, so that the P123 molecules are expected to be present mainly as relatively slow-diffusing micellar aggregates, which may be in equilibrium with a smaller population of relatively rapidly diffusing unimers in solution. As shown in Figure 7b, Peaks 1 and 2 are associated with species with diffusivities that are approximately the same as observed for P123 micelles in aqueous solution ( $D_{\text{P123}}^{\text{P1}}/D_{\text{water}} \approx 0.009$  and  $D_{\text{P123}}^{\text{P2}}/D_{\text{water}} \approx 0.011$ , compared with  $D_{\text{P123}}^{\text{micelle}}/D_{\text{water}} = 0.008$ ). These two peaks are thus attributed to PEO moieties in P123 micellar aggregates, Peak 1 corresponding to PEO not interacting with TPPS<sub>4</sub> (consistent with the  $^1\text{H}\{^{13}\text{C}\}$  HSQC results in Figure 7a, discussed above) and Peak 2 corresponding to PEO interacting with TPPS<sub>4</sub>. Peaks 3 and 4 correspond to PEO moieties in P123 molecules that interact strongly with TPPS<sub>4</sub> dye molecules and exhibit diffusivities that are an order of magnitude larger than those observed for the micellar aggregates ( $D_{\text{P123}}^{\text{P3}}/D_{\text{water}} \approx D_{\text{P123}}^{\text{P4}}/D_{\text{water}} \approx 0.05$ ).

Consequently, Peaks 3 and 4 are attributed to small nonmicellar complexes in solution. The difference in chemical shift between these two peaks may reflect the varying proximity of different  $-\text{CH}_2-$  groups of the PEO block to the associated TPPS<sub>4</sub> dye species, with Peak 4 arising from  $-\text{CH}_2-$  groups closer to the central macrocycle of the porphyrin molecules. The slightly higher diffusivity observed for micellar PEO species interacting with TPPS<sub>4</sub> associated with Peak 2 may result from exchange processes involving these dye-triblock copolymer micellar complexes with the more mobile population of small dye-triblock copolymer complexes in solution represented by Peaks 3 and 4. Thus, in combination with the  $^1\text{H}\{^{13}\text{C}\}$  HSQC spectra in Figures 4 and 7a, b, the PEO  $-\text{CH}_2-$  signals are resolved and assigned as follows: Peak 1 to PEO moieties in P123 micelles without significant interactions with TPPS<sub>4</sub>, Peak 2 to PEO species in P123 micelles interacting with solubilized TPPS<sub>4</sub> guests, and Peaks 3 and 4 to PEO moieties in P123 unimers interacting strongly with TPPS<sub>4</sub> in solution.

Similar HSQC-resolved PG-DSTE diffusion analyses were carried out over the temperature range 5–45 °C to obtain the remaining curves shown in Figure 6. The hollow triangles and squares correspond to the two micellar and unimer triblock copolymer populations discussed above. At temperatures below the CMT of the mixture (20 °C), the same diffusion coefficients are observed for all of the P123 triblock copolymer and TPPS<sub>4</sub> dye species in solution. This suggests, within the sensitivity and resolution limits of the experiment, that all of the dye molecules are associated with small dye-triblock copolymer complexes. As micellization occurs, the P123 species divide into two populations: a fast-diffusing fraction (hollow triangles, solid lines) that exhibits almost the same diffusion coefficient as observed for the dye species over the entire temperature range 5–45 °C and a slow-diffusing fraction corresponding to P123 molecules that have aggregated into micelles (hollow squares, solid lines). The diffusion coefficient of the fast-diffusing fraction was obtained from those P123  $^1\text{H}$  and  $^{13}\text{C}$  HSQC resonances exhibiting the largest chemical-shift changes as a result of the interactions of the triblock copolymer and the dye species, while the diffusion coefficient of the slow-diffusing fraction was obtained from the P123  $^1\text{H}$  and  $^{13}\text{C}$  HSQC signals that revealed little or no direct interactions with the dye species. The similarity between the diffusivities of the fast-diffusing polymer fraction and the TPPS<sub>4</sub> molecules establishes that most of the TPPS<sub>4</sub> molecules are associated with small dye-triblock copolymer complexes even above the critical micellization temperature and over the entire temperature range investigated (5–45 °C). A small fraction of the TPPS<sub>4</sub> molecules is additionally associated with larger micellar P123 aggregates, which accounts for the slightly lower average diffusion coefficients obtained for the dye species, compared to the fast-diffusing P123 fraction. The diffusion behavior of the slow-diffusing fraction was measured to be identical to that obtained in the absence of the dye, i.e., at temperatures below the CMT, a relatively large diffusion coefficient was observed, which decreased rapidly when the CMT was reached and exceeded. For the aqueous TPPS<sub>4</sub>/P123 mixture, however, an approximately 5 °C increase in the CMT was observed compared with aqueous P123 solutions without TPPS<sub>4</sub>, showing that micellization is retarded by the presence of TPPS<sub>4</sub>, although that the size of the micellar aggregates is not affected significantly.

At temperatures above the CMT, it is likely that a dynamic equilibrium exists between small dye-triblock copolymer complexes and larger dye-containing micellar

aggregates. The presence of the charged sulfonate groups of the TPPS<sub>4</sub> dye species increases the hydrophilicity of the dye/polymer complexes. This effect appears to be strong enough to stabilize small P123/TPPS<sub>4</sub> complexes in solution and thereby lead to the significant increase in the CMT (approximately 5 °C for the conditions investigated). This is in contrast to the addition of salts, which typically tend to decrease the micellization temperature by approximately 0.1–10 °C/wt% of salt added.<sup>14,15,17,18,20,93,94</sup> The effect of TPPS<sub>4</sub> complexation with the P123 species is more similar to that induced by the separate addition of surfactants to PEO–PPO–PEO triblock copolymer solutions.<sup>24–27,29,94</sup> This is consistent with the amphiphilic character of the sulfonated TPPS<sub>4</sub> porphyrin molecules, which possess a relatively hydrophobic central macrocycle that interacts strongly with the P123 triblock copolymer species and four highly hydrophilic and negatively charged anionic sulfonate groups that preferentially interact with the aqueous solvent. The porphyrins thus act as compatibilizing agents between the P123 triblock copolymer species and the aqueous solvent. As the hydrophobic character of the triblock copolymer species is increased, for example, as the result of an increase in temperature, the tendency to form micelles becomes stronger and the additional hydrophilicity arising from complexation with the porphyrin molecules eventually ( $T > 20$  °C for the system studied here) becomes insufficient to prevent micellization.

**Dynamic Exchange in TPPS<sub>4</sub>–P123 Mixtures Probed by PG-DSTE <sup>1</sup>H NMR.** On the basis of the analyses of the 2D <sup>1</sup>H{<sup>13</sup>C} HSQC and PG-DSTE diffusion measurements discussed so far, detailed and subtle intermolecular structural information is obtained on the temperature-dependent loci of interactions between the TPPS<sub>4</sub> porphyrin molecules and the different PEO and PPO moieties of the P123 triblock copolymer species. However, as the diffusion data suggest, the resulting structures are dynamic, with molecular exchange occurring among them. For example, such exchange could occur between TPPS<sub>4</sub> dye species associated with small dye–triblock copolymer complexes and dye species solubilized in hydrophilic micellar coronas, in hydrophobic micellar cores, or in free aqueous solution. With the structural relationships among the species unambiguously established, the dynamics and time scales of such exchange processes can subsequently be investigated by performing <sup>1</sup>H PG-DSTE NMR diffusion measurements with varying diffusion times. Such measurements are sensitive to molecular-exchange processes that occur on the order of the diffusion time ( $\Delta$ , typically hundreds of milliseconds to seconds). Species exchanging on these time scales between distinct environments with different diffusion coefficients will give rise to different signal decay behaviors, depending on the diffusion time. If the time scale of a given exchange process is fast compared to the diffusion time, then the observed signal decay will be monoexponential with a diffusion coefficient that is an average of the two environments. If, on the other hand, exchange is comparable to or slower than the diffusion time, the signal will decay biexponentially for a two-site process. The diffusion coefficients and relative populations in both environments can then be determined from a simultaneous multiparameter fit to PGSE diffusion data acquired for several different diffusion times.

Kärger derived relations for such two-site exchange processes for pulsed-gradient NMR diffusion experiments,

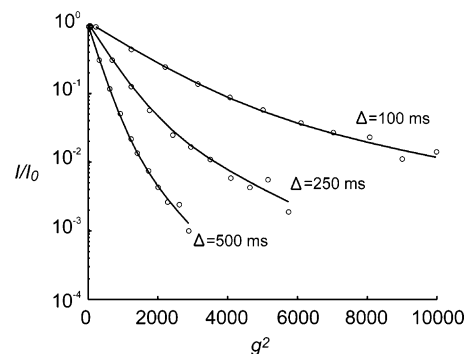


**Figure 8.** Signal decays for the tetra(4-sulfonatophenyl)porphyrin (TPPS<sub>4</sub>) resonances in a 10 mM aqueous solution (pH = 11) of both TPPS<sub>4</sub> and EO<sub>20</sub>–PO<sub>70</sub>–EO<sub>20</sub> (P123) triblock copolymer at 40 °C as functions of gradient strength,  $g$ , and diffusion time,  $\Delta$ , in a series of 1D pulsed-gradient double-stimulated-echo (PG-DSTE) <sup>1</sup>H NMR diffusion experiments. Biexponential decays are observed for all diffusion times examined in the experiment, as determined by nonlinear least-squares fits accompanying the experimental data (solid lines). The resulting values for the diffusion coefficients and residence times, along with estimated standard deviations derived from a Monte Carlo-type error analysis are:  $D_{\text{slow}}/D_{\text{water}} = 0.011 \pm 0.002$ ,  $\tau_{\text{slow}} = 0.4 \text{ s} \pm 0.1 \text{ s}$  and  $D_{\text{fast}}/D_{\text{water}} = 0.048 \pm 0.002$ ,  $\tau_{\text{fast}} = 2.5 \text{ s} \pm 0.9 \text{ s}$ . These values correspond to  $85\% \pm 5\%$  of the TPPS<sub>4</sub> dye molecules being in the faster diffusing state.

as a function of diffusion time,<sup>79,80</sup> that allow the diffusion coefficients ( $D_{\text{slow}}$  and  $D_{\text{fast}}$ ) and average residence times ( $\tau_{\text{slow}}$  and  $\tau_{\text{fast}}$ ) for molecules in each of the two exchanging environments to be established. This is achieved through a simultaneous fit of diffusion data at different diffusion times to these four parameters. The resulting residence times can furthermore be used to estimate the relative populations of the exchanging species (here, the TPPS<sub>4</sub> dye molecules) in the two environments. For example, the fraction of dye molecules exhibiting a slow diffusion coefficient,  $f_{\text{slow}}^{\text{TPPS}_4}$ , is given by

$$f_{\text{slow}}^{\text{TPPS}_4} = \frac{\tau_{\text{slow}}^{\text{TPPS}_4}}{\tau_{\text{fast}}^{\text{TPPS}_4} + \tau_{\text{slow}}^{\text{TPPS}_4}} \quad (1)$$

where  $\tau_{\text{slow}}^{\text{TPPS}_4}$  is the average residence time of the dye molecules in the slow-diffusing micellar environment and  $\tau_{\text{fast}}^{\text{TPPS}_4}$  is the average residence time of the dye molecules in the faster-diffusing small dye–triblock copolymer complexes. This approach was used to model diffusion data obtained from 1D PG-DSTE <sup>1</sup>H NMR measurements of an aqueous solution containing 10 mM concentrations of both TPPS<sub>4</sub> and P123 at 40 °C for three different diffusion times (100, 250, and 500 ms). The selected times spanned a range of time scales relevant for the exchange of TPPS<sub>4</sub> species between different environments. The resulting signal decays are plotted in Figure 8 (circles), as functions of gradient strength,  $g$ , and diffusion time,  $\Delta$ , along with the corresponding four-parameter fit (solid lines). The measurements obtained for the shortest diffusion time, 100 ms, show relatively slow magnetization decay and distinct biexponential character, indicating the presence of two populations diffusing with different rates. As the diffusion time is increased to 250 and 500 ms, the contribution of the faster-decaying, and thus faster-diffusing, component becomes increasingly more important, confirming exchange between the two populations. All three decay curves were simultaneously fit with a single set of diffusivity and residence time parameters for each of the two populations. The corresponding standard deviations, shown in parentheses, were determined by a

(93) Anderson, B. C.; Cox, S. M.; Ambardekar, A. V.; Mallapragada, S. K. *J. Pharm. Sci.* **2002**, *91*, 180–188.

(94) Desai, P. R.; Jain, N. J.; Sharma, R. K.; Bahadur, P. *Colloid Surf. A* **2001**, *178*, 57–69.

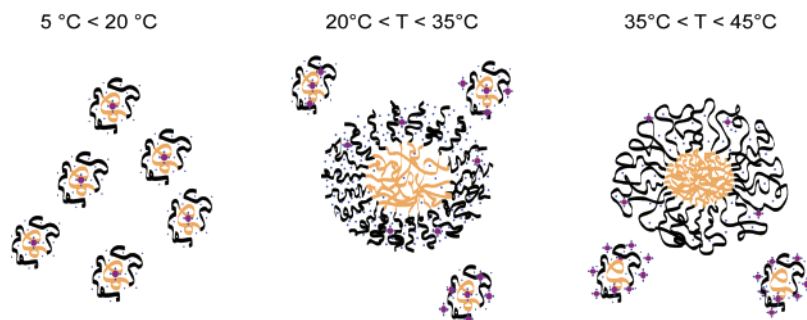


**Figure 9.** Schematic diagram of temperature-dependent micellization and solubilization processes occurring in an aqueous solution (pH = 11) of 10 mM each of tetra(4-sulfonatophenyl)porphyrin (TPPS<sub>4</sub>) and EO<sub>20</sub>-PO<sub>70</sub>-EO<sub>20</sub> (P123) triblock copolymer species. At temperatures above a critical micellization temperature (CMT), the P123 block copolymer complexes to form micelles, while small TPPS<sub>4</sub>-P123 aggregates remain in solution, even above the CMT. The locus of interaction of the TPPS<sub>4</sub> species shifts from the PPO moieties to the PEO moieties of the P123 host species at higher temperatures. The lower and upper temperature bounds correspond to the minimum and maximum temperatures investigated in this study, but the physical limits are likely to be the freezing temperature and the temperature at which macrophase separation of the copolymer and the aqueous solvent occurs.

Monte Carlo-type error analysis. The diffusivities relative to water at 40 °C were found to be  $D_{\text{slow}}^{\text{TPPS}_4}/D_{\text{water}} = 0.011$  ( $\pm 0.002$ ) and  $D_{\text{fast}}^{\text{TPPS}_4}/D_{\text{water}} = 0.048$  ( $\pm 0.002$ ) for the slow-diffusing and fast-diffusing TPPS<sub>4</sub> populations, respectively, while the corresponding residence times were  $\tau_{\text{slow}}^{\text{TPPS}_4} = 0.4$  s ( $\pm 0.1$  s) and  $\tau_{\text{fast}}^{\text{TPPS}_4} = 2.5$  s ( $\pm 0.9$  s), respectively.

The measured TPPS<sub>4</sub> diffusivities correspond well with the values for the different populations of P123 species in micellar and unimer environments obtained from independent <sup>1</sup>H PG-DSTE diffusion measurements of the triblock copolymer components: the P123 micelles were found to have a diffusivity of  $D_{\text{micelle}}^{\text{P123}}/D_{\text{water}} = 0.008$  ( $\pm 0.001$ ), while the small TPPS<sub>4</sub>/P123 complexes were measured to have a diffusivity of  $D_{\text{complexes}}^{\text{P123}}/D_{\text{water}} = 0.045$  ( $\pm 0.002$ ). These close similarities in the relative diffusivities of the TPPS<sub>4</sub> dye molecules and those of the P123 triblock copolymer species obtained from independent measurements support the validity of a two-site exchange model. On the basis of these measurements and analyses using eq 1, 85% ( $\pm 5\%$ ) of the dye molecules are estimated to be associated with the PEO moieties of small TPPS<sub>4</sub>-P123 triblock copolymer complexes at 40 °C, while the remaining 15% are solubilized in the hydrophilic PEO regions of P123 micellar coronas. Such preferential formation of small dye-triblock copolymer complexes most likely arises as a result of both entropic and steric effects. TPPS<sub>4</sub> dye molecules in a micellar environment are expected to be confined near the micelle-water interface because of their relatively high hydrophilicities compared to the P123 block copolymer above its CMT. In such environments, the dye molecules can be expected to possess reduced entropy and to experience greater steric crowding, compared with the dilute and less ordered small dye-triblock copolymer complexes.

From the TPPS<sub>4</sub> diffusion data measured at different diffusion times (Figure 8), it thus appears that, within the sensitivity of the measurements, no dye molecules are present in free aqueous solution. All or nearly all of the dye species appear to be associated with the P123 triblock copolymer host species under the alkaline solution conditions examined. The diffusion data are fit very well with a two-site model, based on TPPS<sub>4</sub> interacting with P123 in micelles or in small molecular complexes. There is no evidence for a faster-diffusing component, with a diffusivity near that of TPPS<sub>4</sub> ions fully solubilized in aqueous solution ( $D_{\text{solution}}^{\text{TPPS}_4}/D_{\text{water}} \approx 0.087$ ), for any of the diffusion times studied. The data thus establish that the slight difference in the average diffusion coefficients of

TPPS<sub>4</sub> determined from 1D <sup>1</sup>H PG-DSTE diffusion measurements using a single diffusion time (Figure 6, solid diamonds) and that determined for small TPPS<sub>4</sub>/P123 complexes from the corresponding polymer resonances using 2D <sup>1</sup>H{<sup>13</sup>C} HSQC-PG-DSTE diffusion measurements (Figure 6, hollow triangles) results from the partitioning of the dye species between micelles and small TPPS<sub>4</sub>-P123 molecular complexes. The partitioning of the TPPS<sub>4</sub> dye species between these different environments follows a relatively straightforward trend in aqueous alkaline (pH 11) solutions: at temperatures below 20 °C, the TPPS<sub>4</sub> molecules are associated nearly exclusively with the PPO moieties in small TPPS<sub>4</sub>-P123 triblock copolymer complexes. As the CMT ( $\sim 20$  °C) is approached and micellization proceeds with increasing temperature, the locus of principal TPPS<sub>4</sub> interactions changes to the PEO moieties of the P123 species. Most of the TPPS<sub>4</sub> molecules retain strong interactions with and stabilize the small dye-triblock copolymer complexes, although a minor fraction (on the order of 15%) interacts strongly with and is solubilized in self-assembled P123 triblock copolymer micelles.

## Conclusions

A schematic diagram is shown in Figure 9 that summarizes the results and analyses of the TPPS<sub>4</sub>-P123 interactions and micellization processes that occur in an aqueous alkaline solution of TPPS<sub>4</sub> and P123 triblock copolymer species. At temperatures below 20 °C, when both the PEO and PPO blocks are significantly hydrated, the TPPS<sub>4</sub> species, in particular the unprotonated pyrrole nitrogen atoms of the central porphyrin macrocycle, interact most favorably with the PPO moieties. The majority of the dye species experience relatively strong interactions with the propylene oxide blocks of P123 unimers, as evidenced by the correlated changes in the <sup>1</sup>H and <sup>1</sup>H{<sup>13</sup>C} HSQC-resolved chemical shifts of these components upon mixing, the strong <sup>1</sup>H ROE signals observed, and the equivalent diffusion coefficients measured for the two species. As the temperature is increased above the CMT of the mixture (20 °C), the locus of interaction of the hydrophilic TPPS<sub>4</sub> dye molecules shifts from the PPO blocks to the PEO blocks, as evidenced by reduced perturbation of the PPO resonances in <sup>1</sup>H and <sup>1</sup>H{<sup>13</sup>C} HSQC spectra, increased perturbation of the PEO resonances in <sup>1</sup>H{<sup>13</sup>C} HSQC spectra, and changes in the corresponding <sup>1</sup>H ROE cross-relaxation peaks. It thus appears that over the temperature range 20–35 °C, TPPS<sub>4</sub> dye molecules experience energetically favorable inter-

actions with both the PEO and the PPO moieties, modulated by the different temperature-dependent hydrophilicities of the copolymer blocks. As the hydrophobicity of the PPO block increases with increasing temperature (20–35 °C), the favorable interactions between the TPPS<sub>4</sub> dye species and the PPO moieties become increasingly offset by the high relative hydrophilicities of the charged sulfonate groups of the TPPS<sub>4</sub> dye species. As a result, the locus of interaction of the dye species shifts to the PEO moieties, which remain significantly hydrated. The increased hydrophobicity of the PPO blocks induces micellization of the P123 triblock copolymer species, as evidenced by calorimetric measurements and by the more than 3-fold decrease in the P123 diffusion coefficient measured over the range of 20–35 °C. A further consequence of the strong interactions between the TPPS<sub>4</sub> dye molecules and the P123 triblock copolymers species in TPPS<sub>4</sub>/P123/D<sub>2</sub>O solutions is that the onset temperature for P123 micellization is increased by approximately 5 °C to a CMT of 20 °C, compared with 15 °C for alkaline P123/D<sub>2</sub>O solutions. At temperatures above the CMT, a dynamic equilibrium exists between dye molecules interacting principally with the PEO moieties of the triblock copolymer in micelles or in small dye–triblock copolymer complexes, with the majority of the dye molecules associated with the latter. On the other hand, most of the P123 species are present in the form of micelles at these temperatures (> 20 °C), as reflected by the relative signal intensities in <sup>1</sup>H{<sup>13</sup>C} HSQC spectra.

The results establish that different temperature-dependent interactions between small-molecule guest species and different moieties of a self-assembling triblock copolymer host can be balanced to control the distribution of guest species in aqueous solutions. For the TPPS<sub>4</sub>/EO<sub>20</sub>–PO<sub>70</sub>–EO<sub>20</sub> system considered here, the temperature-dependent hydrophobicity of the PPO moieties relative to the PEO moieties in pH 11 alkaline solutions was used

to direct the water-soluble porphyrin guest molecules toward selective interactions with either the PEO or the PPO blocks. Such considerations and the spectroscopic methods by which they have been elucidated should be generally applicable to a wide range of guest molecules in similar micellar solutions, including organic molecules for drug delivery applications.

These conclusions have been made possible by combining several powerful NMR spectroscopy techniques, such as pulsed-gradient diffusion measurements, <sup>1</sup>H{<sup>13</sup>C} heteronuclear correlation experiments, and <sup>1</sup>H NOE/ROE methods. These provide substantially more resolution, and thus insight, than has previously been possible to obtain on host–guest interactions at a molecular level. In particular, the incorporation of 2D <sup>1</sup>H{<sup>13</sup>C} heteronuclear correlation pulse sequences into <sup>1</sup>H NMR diffusion measurements permit much more detailed, robust, and self-consistent analyses of the structures, dynamics, and effects of guest–host interactions on the phase behavior of the self-assembling triblock copolymer species. The resulting insights are expected to lead to improved design and processing of heterogeneous self-assembled systems in a variety of areas, including more-efficient drug delivery systems and superior organic–inorganic materials for optical applications.

**Acknowledgment.** The authors thank Prof. J. Ribó (Universitat de Barcelona) for helpful discussions. This work was supported in part by U.S. National Science Foundation under award DMR-02-33728, by the MRSEC Program through the UCSB Materials Research Laboratory of the National Science Foundation under award DMR-00-80034, and by the USARO through the UCSB Institute for Collaborative Biotechnologies.

LA048435D